Local fluctuations and ordering in liquid and amorphous metals

S.-P. Chen*
Department of Physics, University of Pennsylvania, Philadelphia, Pennsylvania 19104-6396
and Laboratory for Research on the Structure of Matter, University of Pennsylvania, Philadelphia, Pennsylvania 19104-6202

T. Egami and V. Vitek
Department of Materials Science and Engineering, University of Pennsylvania, Philadelphia, Pennsylvania 19104-6272
and Laboratory for Research on the Structure of Matter, University of Pennsylvania, Philadelphia, Pennsylvania 19104-6202
(Received 23 April 1987; revised manuscript received 7 July 1987)

A molecular-dynamics study of the structure and dynamics of monatomic liquids and glasses is presented. The local atomic structure and its development during the quenching process are analyzed in terms of fluctuations of atomic-level stresses and their correlations. This approach extends the basis for the description of the local structure from the usually employed scalar quantity, the local density fluctuation, to a tensorial quantity, the local stress fluctuation. It is shown here that the local stress fluctuations and their spatial and temporal correlations provide a detailed picture of the dynamics of the liquid and of the transition from an ideal fluid to a viscous liquid, and then to a glass. In particular, it is demonstrated that the shear stresses which are spatially uncorrelated at high temperatures become correlated below a temperature, T_s, which is about twice the glass transition temperature. At the same time the dynamic behavior of the liquid, characterized by the diffusivity, viscosity, and phonon states, changes sharply at this temperature. Implications of this apparent structural transition and its origin are then discussed.

I. INTRODUCTION

The structure of liquids and amorphous metals and their dynamics have been a subject of a large number of theoretical and computer-simulation studies.[1-5] The structure of liquids is usually described in terms of local density fluctuations, and their dynamics has often been investigated in the framework of hydrodynamic theories.[1] Initially, only linear approximations were considered, but the modern mode-coupling theory employs nonlinear equations and incorporates thus, to some extent, the atomistic nature of the system.[6,7] This theory was recently extended to describe even the glass transition[8-10] but it does not explain satisfactorily several phenomena observed experimentally or in computer-simulation studies. For instance, while it describes successfully the power law for the long tail of the velocity or shear stress autocorrelation functions, it does not give correct magnitudes of the long tail.[11] It also predicts that just above the glass transition temperature T_g the viscosity should obey a power law.[12,13] However, while such a power law has been observed experimentally, it breaks down at a temperature much higher than T_g.[14]

Such discrepancies indicate that the glass transition is not described adequately in the framework of hydrodynamic theories. In order to make further progress a more detailed understanding of atomic-level mechanisms need to be developed, and for this purpose it may be necessary to adopt a different point of view in describing the local structure. In this paper we introduce such an alternative approach which is based upon the notion of atomic-level stresses. The basis for the description of the local structure is thus extended from the usually employed scalar quantity, the fluctuation of the local density, to a tensorial quantity, the fluctuation of the local stress. This description of the local structure includes density fluctuations since they are represented by the hydrostatic component of the stress tensor, but treats on an equal footing the local shear strain fluctuations, represented by shear stresses. The local density fluctuations are related to the local atomic coordination number, while the shear strains relate to local distortions away from the spherical symmetry in the near-neighbor coordination shells.

To demonstrate these concepts and show their physical significance we present here results of a molecular-dynamics study of a monatomic liquid as it is gradually cooled down from a relatively high temperature and subsequently passes through the glass transition without crystallization. The analysis of the structure in terms of the local density and shear fluctuations leads to a new interpretation of both the glass transition and the dynamics of liquids. In particular, it has been suggested earlier that the thermal averages of the second moments of the stresses are proportional to temperature at high temperatures, but freeze to finite values at the glass transition.[15] The validity of this hypothesis is first demonstrated in this work. It is further shown here that spatial correlations of the local shear stresses develop well above T_g as a result of the increase in viscosity, and it is suggested that the percolation of correlated regions leads then to the glass transition. The onset of these correla-

tions appears to be rather well defined, and it may mark another structural transition in the liquid state, although an establishment of this hypothesis needs further investigations.

II. ATOMIC-LEVEL STRESSES

An important tensorial quantity characterizing the internal state of matter is the stress. Its significance in both classical[16] and quantum systems[17–19] has been recognized for a long time, and in studies of the stability and dynamics of crystal lattices the concept of stress was first employed by Born and Huang.[20] Following the arguments analogous to those used in the derivation of the force theorem, usually attributed to Hellmann and Feynman,[21] it has been shown by Nielsen and Martin[22] that the total stress in a system $\sigma^{\alpha\beta}$, where α and β are the Cartesian coordinates, can be defined as the expectation value of the linear term in the expansion of the Hamiltonian with respect to an infinitesimal virtual strain $\epsilon^{\alpha\beta}$. A hydrodynamic quantity which differentiates glass from liquid, the shear viscosity η, is given in terms of the total shear stresses by the Green-Kubo formula[1]

$$\eta=\frac{V}{k_B T}\int_0^\infty \langle \sigma^{\alpha\beta}(0)\sigma^{\alpha\beta}(t)\rangle dt \quad (\alpha\neq\beta) , \tag{1}$$

where $\langle\ \rangle$ indicates the thermal average, $\sigma^{\alpha\beta}(t)$ is the total shear stress at the time t, V is the volume, T is the temperature, and k_B is the Boltzmann constant.

The total stress can be broken up into local atomic-level stresses in such a way that the total stress can be written as the following sum:

$$\sigma^{\alpha\beta}=\frac{1}{V}\sum_i \Omega_i \sigma^{\alpha\beta}(i) , \tag{2}$$

where Ω_i is the volume associated with the atom i, for instance the volume of the corresponding Wigner-Seitz cell (Voronoi polyhedron), and $\sigma^{\alpha\beta}(i)$ is the $\alpha\beta$ component of the atomic-level stress at the atom i. The atomic-level stress is then the local response of the system to the virtual strain $\epsilon^{\alpha\beta}$, and if the total potential energy of the system can be written as a function of separations between the atoms, it can be easily shown that the tensor of the atomic-level stresses is

$$\sigma^{\alpha\beta}(i)=-\frac{1}{\Omega_i}\left[\tfrac{1}{2}\sum_j F_{ij}^{\alpha} r_{ij}^{\beta}+M_i v_i^{\alpha} v_i^{\beta}\right] , \tag{3}$$

where $\mathbf{r}_{ij}$ is the separation of atoms i and j, $\mathbf{F}_{ij}$ is the force on atom i due to atom j, M_i is the mass of the atom i, and $\mathbf{v}_i$ is the velocity of this atom. If the atomic interactions are approximated by a central force potential $\Phi(r_{ij})$, as is done in the MD studies presented here, $F_{ij}^{\alpha}=-(d\Phi/dr_{ij})(r_{ij}^{\alpha}/r_{ij})$. For any given atom $\sigma^{\alpha\beta}(i)$ is a nonlocal function of the state of matter in the vicinity of this atom, since the interactions, described for example by Φ, have a finite range. This is in contrast with the local character of the stress field as used in the usual elasticity theory.

Since in liquids and glasses the environment of any atom has a spherical symmetry on average, though not at every locality and at all times, it is convenient to define the atomic-level stresses in terms of spherical harmonics as

$$\sigma_l^m(i)=\frac{1}{\Omega_i}\left[\sum_j \frac{1}{2}\frac{d\Phi}{dr_{ij}} r_{ij} Y_l^m(\hat{\mathbf{r}}_{ij})-M_i v_i^2 Y_l^m(\hat{\mathbf{v}}_i)\right] . \tag{4}$$

Here the $l=0$ component describes the hydrostatic pressure, p, since

$$p_i=\left[\frac{4\pi}{9}\right]^{1/2}\sigma_0^0(i) , \tag{5}$$

while the $l=2$ components describe shear stresses. In particular the rms of the shear stresses,

$$\tau_i=\left[\frac{4\pi}{15}\right]^{1/2}\left[\sum_{m=-2}^{2}|\sigma_2^m(i)|^2\right]^{1/2} , \tag{6}$$

is the von Mises shear stress which is a commonly used measure of average shear stresses.[23]

The atomic-level stresses as defined above have been successfully used in describing the atomistic nature of defects in crystalline solids, for example cores of dislocations.[24] The usefulness of the atomic-level stresses for the description of the structure of glasses was first demonstrated by Egami *et al.*[25] Several properties of metallic glasses, including the structural relaxation phenomena,[26,27] mechanical deformation,[28] and glass transition[15] have been treated successfully using this concept. The local hydrostatic pressure describes the local density fluctuation, and is approximately linearly related to the local coordination number.[29,30] The local volume strain e_i^v could then be defined as

$$e_i^v=p_i/B_i , \tag{7}$$

where B_i is the local bulk modulus.[30] On the other hand, the shear stresses describe the deviation of the local environment of an atom from the spherical symmetry, and the directions of the principal stresses indicate the axes of such local distortions. The average local shear strain can be defined as

$$e_i^{\tau}=\tau_i/2G_i , \tag{8}$$

where G_i is the local shear modulus. Computer simulations of single-component and binary metallic glasses showed that the rms value of the local volume strain was as large as 6% and of the local shear strain about 10%.[26,27,30]

The atomic-level stresses defined here describe the local structural fluctuations and distortions, but they are not simple topological variables because they include the interatomic interactions and thus the energetics of the local environment in their definition. For this reason it may be easier to relate physical properties to these stresses than to purely topological characteristics of the local environment such as Voronoi polyhedra or Bernal holes, commonly used for the description of the local environment.

III. MOLECULAR-DYNAMICS SIMULATION

A molecular-dynamics (MD) study of a monatomic liquid was carried out using a model containing about 900 particles interacting via the modified Johnson potential. This is a short-range pair potential known to reproduce many of the properties of bcc iron.[30,31] Relevant characteristics of this potential are listed in Table I. We used the microcanonical MD algorithm of Beeman[32] and Sangster and Dixon[33] which conserves the total energy better than the earlier argorithms. The time step was chosen to be 10^{-15} sec, which is $\frac{1}{100}$ of the Debye time for this system (1.02×10^{-13} sec); the relative energy fluctuation per step was then less than 10^{-5}. The temperature of the system was calculated from the kinetic energy assuming the equipartition principle. An initial state was produced by placing atoms with zero velocity randomly into a cube until the specified density was achieved. After about 100 MD steps a Maxwellian distribution of velocities was attained, and the temperature of the system was about 3400 K. The system was then cooled in alternating quenching steps (consisting of 10^2-10^3 MD steps) and equilibriating steps (consisting of 10^3-10^4 MD steps). The volume of the system was kept constant during the calculation. The details of three different MD calculations performed are summarized in Table II. Various temperature-dependent properties such as the average stresses and their correlation functions, were always evaluated during the last 10^2-10^3 MD steps of each equilibrating step. In one case, marked run A, the system was first cooled down to 0 K and then warmed up in the reverse process. Long MD runs up to 8×10^4 steps were added to many of the temperature steps of the run C, in order to calculate the diffusivity and to observe the effect of structural relaxation as discussed later. Preliminary results of these studies have been presented in two papers.[34]

In a separate MD run we observed the system crystallize into the body-centered-cubic lattice. Although crystallization and melting are not the subject of the present paper this observation is worth mentioning, since it assures that all the results discussed further are not due to partial crystallization. This MD run started at 1220 K and crystallization was noted by a rapid increase in temperature and a change in the pair distribution function (PDF). The temperature of the system was increasing as the crystallization proceeded, since in the microcanonical system the latent heat released during crystallization could not dissipate. The PDF after 5×10^4 MD steps, when the temperature increased to 1320 K, is shown in Fig. 1(a). Clearly, at this stage the bulk of the sample was still liquid although crystallization must have started. Within the next 2000 MD steps the temperature of the system rapidly increased to 1620 K, accompanied by a drastic change in the PDF. Additional MD relaxation did not lead to any further significant changes, and the PDF after total of 7×10^4 MD steps is shown in Fig. 1(b). This PDF corresponds to a vibrating bcc crystal. In addition, we carried out similar MD studies on a bcc system consisting of 1024 atoms. Upon heating this system showed increased disorder above the experimental melting temperature (1808 K), but did not quite lose the crystalline structure, judging according to the PDF. In other words, it did not totally melt, presumably because the volume was kept constant.

TABLE I. Some properties of the modified Johnson potential (Ref. 30).

Position of the minimum:	2.617 Å
Depth of the minimum:	−0.252 eV
Curvature at the minimum:	1.915 eV/Å^2

TABLE II. Data on the MD runs.

Symbol	No. of atoms	Quenching rate (K/step)	Quenching steps	Equilibriating steps
A	875	2	100	1000
B	884	2	100	1000
C	884	0.2	1000	(1×,3×,5×)10000
D	2067			relaxed statically by the steepest-descent method

IV. TEMPERATURE DEPENDENCE OF PRESSURE AND SHEAR STRESS FLUCTUATIONS

The temperature dependence of the average pressure per atom, $\langle p \rangle$, for three of the MD runs is shown in

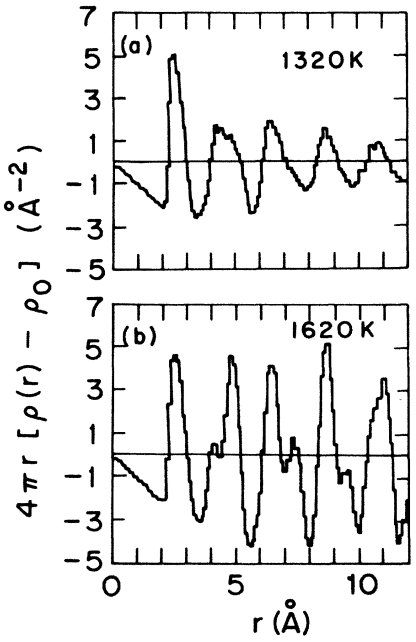

FIG. 1. (a) PDF after 5×10^4 MD steps when the temperature increased to 1320 K (just before crystallization). (b) PDF after 7×10^4 MD steps when the system is already crystalline and the temperature increased to 1620 K.

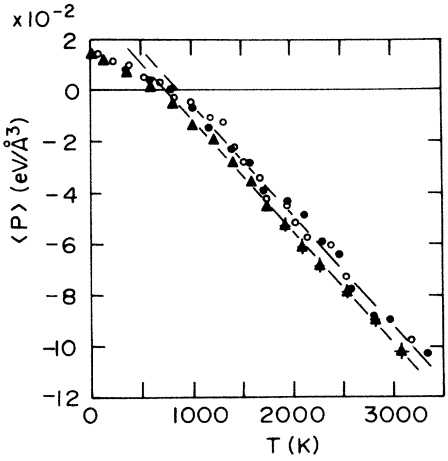

FIG. 2. Temperature dependence of the average pressure $\langle p \rangle$. Run A (cooling), solid circles; run A (heating), open circles; run C, solid triangles.

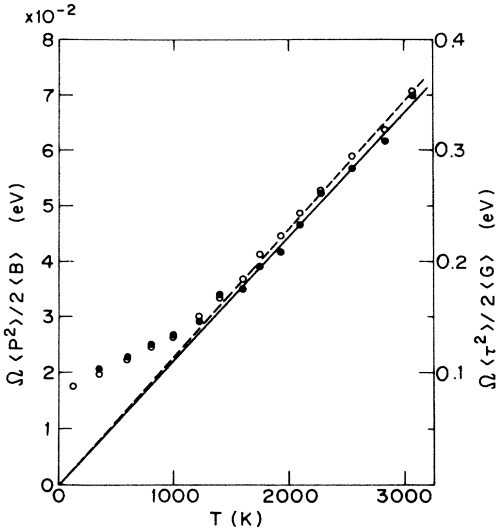

FIG. 3. Temperature dependence of the "elastic self-energies" per atom $\Omega\langle p^2 \rangle/2\langle B \rangle$ (open circles) and $\Omega\langle \tau^2 \rangle/2\langle G \rangle$ (solid circles).

Fig. 2. The result for run B is very similar to that for run C and is not shown here. As mentioned earlier, the system remained supercooled without crystallization even below the melting temperature of the crystal. However, there is a clearly defined change in the slope of the $\langle p \rangle$ versus T dependence at around 900 K, which we interpret to indicate the glass transition. Tentatively, we call this temperature T_g. The variation of $\langle p \rangle$ with temperature is, of course, a direct consequence of keeping the volume constant. If we assume that the system responds elastically to the change in volume, the expected thermal expansion coefficient for the case of constant pressure is given by $-(\partial\langle p \rangle/\partial T)/3B$, where B is the bulk modulus. Below T_g it is 2×10^{-5}, while it is 5×10^{-5} above T_g, confirming that the change in the slope in Fig. 2 implies the glass transition. Since we are mostly concerned with the distribution of the local pressure rather than its average, this average value will always be subtracted from the local pressure in the results presented in the remainder of this paper.

The temperature dependences of the second moments of the pressure and shear stress fluctuations, $\langle p^2 \rangle$ and $\langle \tau^2 \rangle$, are seen from Fig. 3. In this figure the elastic self-energies per atom, $\Omega\langle p^2 \rangle/2\langle B \rangle$ (open circles) and $\Omega\langle \tau^2 \rangle/2\langle G \rangle$ (solid circles), where Ω is the average volume per atom and $\langle B \rangle$ and $\langle G \rangle$ are the volume averages of local instantaneous bulk and shear modulus, respectively, are plotted as functions of temperature. However, since both the bulk and shear modulus have been found to be almost independent of temperature, the dependence of the self-energies on temperature is practically the same as that of $\langle p^2 \rangle$ or $\langle \tau^2 \rangle$. At high temperatures this dependence is linear but a deviation from linearity occurs at lower temperatures, and both $\langle p^2 \rangle$ and $\langle \tau^2 \rangle$ freeze to some finite values at very low temperatures as suggested earlier.[15] The deviation from linearity starts, however, well above T_g, at around 1600 K. We tentatively call this temperature the shear transition temperature, T_s, and its meaning is discussed in more detail in Sec. VI. The elastic self-energies follow closely a linear dependence on T at high temperatures, as expected,[15] and they are approximately equal to $\frac{1}{4}k_BT$ and $\frac{5}{4}k_BT$ for pressure and shear stresses, respectively. Thus the potential energy of the system, equal according to the equipartition theorem to $\frac{3}{2}k_BT$, appears to be divided equally among the six components of the stress tensor.

V. VISCOSITY, DIFFUSIVITY, AND VIBRATIONAL STATES

In order to gain an insight into the dynamic properties of the system studied, the shear stress autocorrelation function

$$S(t)=\sum_{m=-2}^{2}\langle \sigma_2^m(0)\sigma_2^{-m}(t)\rangle\ , \tag{9}$$

the time integral of which determines viscosity [see Eqs. (1) and (4)], was calculated at various temperatures and results are shown in Fig. 4. At high temperatures, for instance at 3083 K, $S(t)$ decreases rapidly within one Debye time (1.02×10^{-13} sec) and then fluctuates around zero. Below T_g, for example at 590 K, it remains high after an initial drop, resulting in a very high viscosity. The existence of this large tail leads to a rapid increase of viscosity with decreasing temperature in the supercooled liquids. However, it is noteworthy that at intermediate temperatures, $T_g < T < T_s$, $S(t)$ does decrease but not as rapidly as above T_s, as seen in Fig. 4 from the curve for $T=1408$ K. Such a long tail was observed also in the MD simulation by Levesque *et al.*[3] near the triple point of argon. The shear viscosity was evaluated by integrating $S(t)$ after it has been fitted by two exponential functions. This estimate is, however, unreliable below 1000 K, since the tail of $S(t)$ becomes

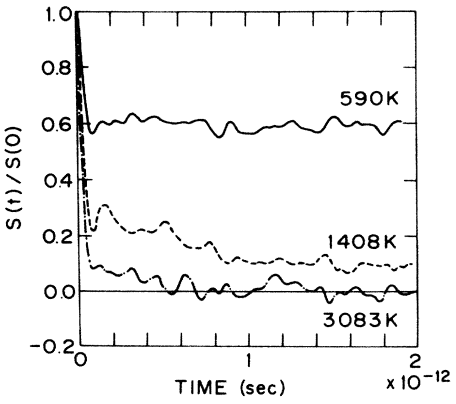

FIG. 4. Shear stress autocorrelation function at temperatures 3083, 1408, and 590 K.

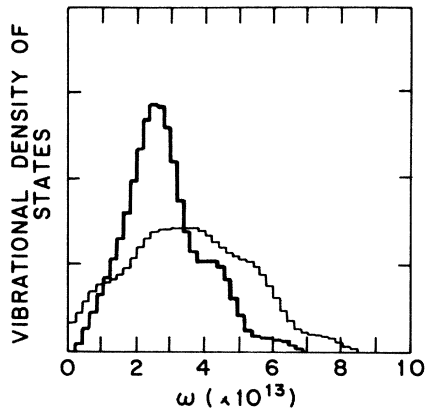

FIG. 6. Total vibrational density of states at $T=2100$ K (thin lines) and $T\simeq 3$ K (bold lines).

too long. We find the value of η at T_s to be 0.16 P, and the Maxwell shear relaxation time $\eta/\langle G\rangle$ to be 2×10^{-13} sec. Therefore the system is definitely a liquid at T_s, and it is clear that T_s does not signify the glass transition, even though the MD runs have been done for relatively short real times, up to 5×10^{-11} sec.

We have also calculated the diffusivity, D, from the atomic displacements, by plotting $\langle[r(t)-r(0)]^2\rangle$ against time, where $r(t)$ is the position of an atom at a time t. As shown in Fig. 5, D exhibits an Arrhenian behavior at high temperatures, with the activation energy of 0.58 eV, which compares favorably with experimental data[35] (0.53 eV). However, below T_s it deviates from the Arrhenian dependence, and as shown in Fig. 5, exhibits a relaxation behavior: diffusivity decreases with time as the system becomes more relaxed. Furthermore, it was found that down to about 1000 K, the diffusivity and viscosity approximately satisfy the Stokes-Einstein relation,

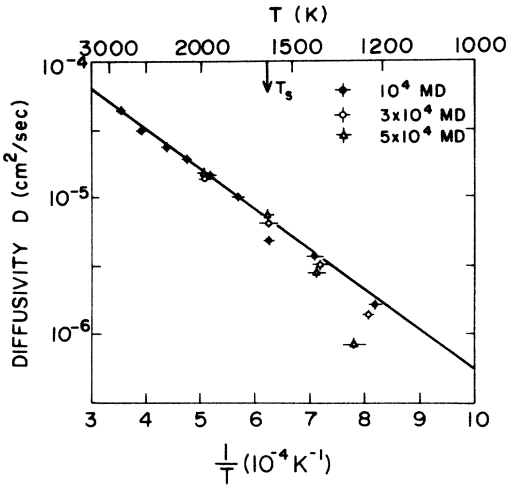

FIG. 5. Temperature dependence of the diffusivity D.

$$\eta D/kT=1/6\pi a\ , \tag{10}$$

where a is about 1.3 Å, which agrees well with the atomic radius of iron which is one of the parameters to which the pair potential used here has been fitted. In addition we have calculated the total phonon density of states from the velocity autocorrelation functions. As shown in Fig. 6 the phonon density of states at low temperatures is characterized by two peaks corresponding to transverse and longitudinal waves, respectively. As the temperature is raised the low-frequency transverse-phonon peak becomes weaker, but it has been found that the peak height changes smoothly through T_g and it disappears only above T_s. Therefore, the viscous liquid in the temperature range between T_g and T_s can support significant density of shear phonons. The high-frequency peak, which is due to longitudinal phonons, remains largely unchanged with temperature, as expected.

VI. SPATIAL CORRELATION OF SHEAR STRESSES

The deviation of $\langle p^2\rangle$ and $\langle\tau^2\rangle$ from a linear dependence on temperature, the long tail in the autocorrelation function of the shear stresses, the deviation of the diffusivity from the Arrhenian temperature dependence, and the appearance of transverse phonons, all of which occur at temperatures close to T_s, indicate that some structural changes are taking place at T_s. In particular, the deviation of the elastic self-energies away from the linear dependence on T implies that local stresses evaluated at individual atoms are no longer independent below T_s, and some spatial correlations are likely to be developing. We have, therefore, evaluated the following spatial correlation factors for shear stresses:

$$S_l(n\mathrm{NN})=\sum_{i,j}S_{i,j}(2,2,l)/N_pS_{\max}(2,2,l)\ , \tag{11}$$

where sums over i and j are taken for pairs of atoms which are nth-nearest neighbors (nNN) to each other and

$$S_{i,j}(2,2,l)=\frac{\sum_{m_1,m_2,m_3}(-1)^{l/2}\begin{pmatrix}2&2&l\\m_1&m_2&m_3\end{pmatrix}\langle\sigma_2^{m_1}(i)\sigma_2^{m_2}(j)Y_l^{m_3}(\hat{\mathbf{r}}_{ij})\rangle}{\sum_m\langle|\sigma_2^m(i)|^2\rangle}, \tag{12}$$

where the term in large parentheses is the Wigner $3j$ symbol. N_p is the number of pairs of atoms in the summation in Eq. (11) and $S_{\max}(2,2,l)$ is the maximum possible value of $S_{i,j}(2,2,l)$; this was evaluated by considering a pair of atoms with identical principal values of the atomic-level stresses. Here the neighbors were defined according to the peaks in the radial distribution function. In the model we used, the first-nearest neighbors (1NN) are all the atoms at interatomic distances $r_{ij}\leq 3.44$ Å; for the second-nearest neighbors (2NN) $3.44<r_{ij}\leq 5.7$ Å, for the third-nearest neighbors (3NN) $5.7<r_{ij}\leq 7.9$ Å, for the fourth-nearest neighbors (4NN) $7.9<r_{ij}\leq 10.0$ Å, and for the fifth-nearest neighbors (5NN) $10.0<r_{ij}\leq 12.2$ Å.

For the nearest neighbors we found that S_2(1NN) shows a strong temperature dependence as shown in Fig. 7, while correlation functions for other values of l are only weakly temperature dependent as shown in Fig. 8. In Fig. 7, S_2(1NN) is seen to start increasing rapidly below 1500–1600 K, i.e., at temperatures close to T_s. Above T_s the value of S_2(1NN) is practically constant, approximately equal to 0.08. For the second-nearest neighbors and beyond, it was found that S_4(2NN), rather than S_2(2NN), exhibits a strong temperature dependence as shown in Fig. 9, while other correlation factors remain nearly constant. The fourfold correlation, $S_4(n\text{NN})$, was found to extend at least up to the fifth-nearest neighbors. Above T_s all the stress correlation parameters other than those for the nearest neighbors are essentially zero, indicating that the stresses are spatially uncorrelated. For the nearest neighbors the correlation parameters will not be zero even in the absence of any real correlation because the force between two neighboring atoms contributes simultaneously to the stresses on these sites. More specifically, if in Eq. (4) quantities such as $d\Phi/dr_{ij}$ and $Y_l^m(\hat{\mathbf{r}}_{ij})$ are totally uncorrelated at high temperatures, the shear stress correlation function for atom i and atom j which are nearest neighbors to each other becomes

$$\langle\sigma_2^m(i)\sigma_2^{m'}(j)\rangle\sim\frac{1}{4\Omega_i\Omega_j}\left\langle\left[r_{ij}\frac{d\Phi}{dr_{ij}}Y_2^m(\hat{\mathbf{r}}_{ij})\right]^2\right\rangle\delta_{m,m'}, \tag{13}$$

while

$$\langle[\sigma_2^m(i)]^2\rangle\sim\frac{1}{4(\Omega_i)^2}\sum_j\left\langle\left[r_{ij}\frac{d\Phi}{dr_{ij}}Y_2^m(\hat{\mathbf{r}}_{ij})-2M_i(v_i)^2Y_2^m(\hat{\mathbf{v}}_i)\right]^2\right\rangle. \tag{14}$$

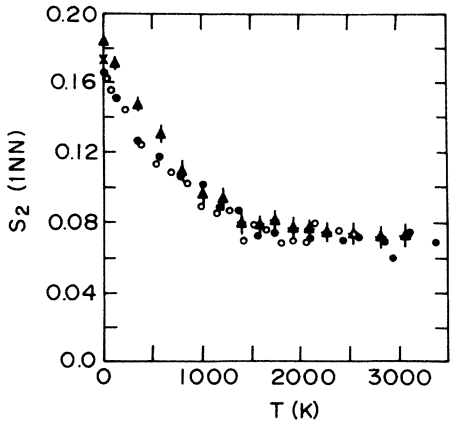

FIG. 7. Temperature dependence of the stress correlation parameter S_2(1NN) for the first-nearest neighbors. Notation used for individual runs is the same as in Fig. 2; × corresponds to the run D.

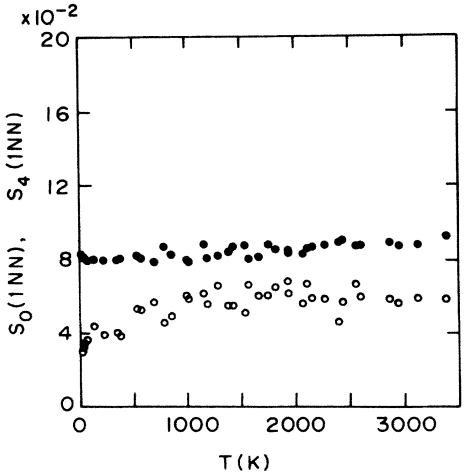

FIG. 8. Temperature dependence of the stress correlation parameters S_4(1NN) (solid circles) and S_0(1NN) (open circles) for the first-nearest neighbors.

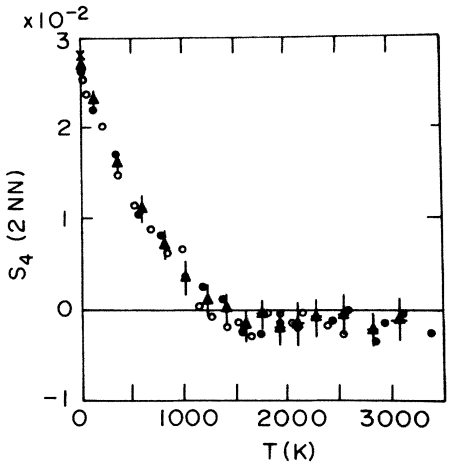

FIG. 9. Temperature dependence of the stress correlation parameter $S_4(2NN)$ for the second-nearest neighbors. Notation used for individual runs is the same as in Figs. 2 and 7.

Thus, if the kinetic contribution [the second term in (14)] is small,

$$\langle \sigma_2^m(i)\sigma_2^{m'}(j)\rangle / \langle [\sigma_2^m(i)]^2\rangle \sim \frac{1}{Z}\delta_{m,m'}, \quad (15)$$

where Z is the average coordination number equal to 12.5. Therefore, $S_2(1NN) \sim S_4(1NN) \sim 0.08$ for $T > T_s$ in agreement with our MD results. Thus, it can be concluded that the shear stresses are uncorrelated above T_s, but show considerable spatial correlations below T_s.

The correlation parameters $S_2(1NN)$ and $S_4(2NN)$ were calculated for all the MD runs listed in Table I, as well as for a statically relaxed structure consisting of 2067 atoms (run D).[25,29] The results are all in agreement suggesting that these parameters do not depend upon the details of the relaxation procedure, nor significantly reflect the small difference in the density of the two models (run A and runs B and C). Our parameters are also insensitive to the extent of the relaxation. They reach equilibrium values within 10^3 MD steps, and do not change appreciably even when the diffusivity changes with time due to structural relaxation. On the other hand, they exhibit rapid and large changes when the system crystallizes, as shown in Fig. 10. Note that the sign of $S_4(2NN)$ for the glass is opposite to that for the crystal. Thus it is clear that the increase in $S_4(n\text{NN})$ at low temperature is not due to an incipient crystallization.

VII. DISCUSSION

The results of the MD simulation of a monatomic liquid show that stresses evaluated at individual atom positions are independent of each other at high temperatures. However, certain spatial correlations develop below a temperature T_s at which various changes in the dynamic properties of the system also occur. In the following we discuss first the origin of these atomic-level stresses and their correlations, and then consider implications of these correlations for various physical properties of supercooled liquids and glasses.

As alluded to in Ref. 30, the origin of the atomic-level stresses is the misfit between the size and shape of an atom and the size and shape of the "hole" made by its neighboring atoms. For instance, an ideal icosahedral cluster can be formed from 13 atoms only when the size of the central atom is about 91% of that of the atoms on its surface. This is because in the icosahedron the distance from its center to any vertex on the surface is shorter, by about 5%, than the distance between the neighboring vertices on the surface. Consequently, if an icosahedron is formed by 13 atoms of equal size, the atom at the center would be under compression. A computer simulation of a dense random packed (DRP) structure[29] indeed showed that in this structure the atoms surrounded by 12 nearest neighbors which form icosahedra are mostly under a compressive stress, while atoms with more than 13 neighbors are largely under tension. Similarly, if neighboring atoms are configured in a manner distorted away from the spherical symmetry a shear stress is produced when an atom is placed into the corresponding hole.

Owing to these features of icosahedral clusters of atoms, if one attempts to construct a disordered structure by packing only tetrahedra of atoms, thus locally forming icosahedra, stresses in this structure would rapidly increase with the size of the aggregate. In order to remove such stresses, Kléman and Sadoc introduced the notion of the curved space.[36] They pointed out that at a certain curvature the space can be filled by tetrahedra alone without any distortions, and such a structure may then be used as a template for the structure in the real, flat (Euclidean) space.[37,38] The real structure is then

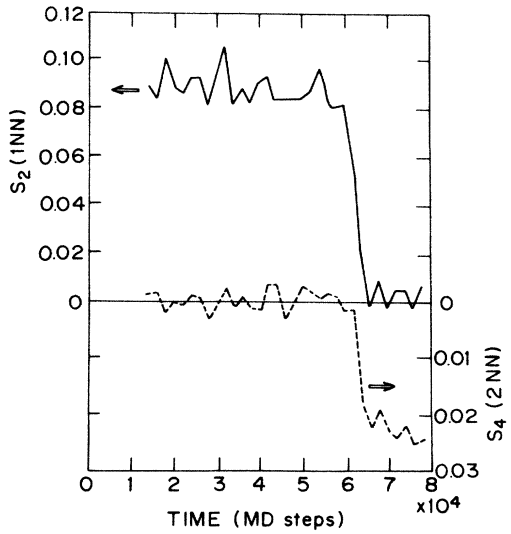

FIG. 10. Dependence of $S_2(1NN)$ and $S_4(2NN)$ on time (in units of MD steps) showing the changes of these correlation parameters which are occurring during crystallization at $T = 1320$ K (cf. Fig. 1).

produced by introducing appropriate disclinations into the structure in the curved space such that mapping onto the flat space can be performed. Nelson developed this idea further into a general theory of the structure of glasses by investigating the nature of these disclinations.[39,40] While stresses are not explicitly considered in these models, they arise naturally as a consequence of bringing the structure from the curved space to the flat space.

The misfit between the atom and its surrounding, however, not only produces a stress at its position, but also a long-range stress field around it. The presence of such a long-range stress field has been confirmed through the analysis[27] of the experimentally observed structural changes during the structural relaxation.[41] Obviously, the local stress at a misfitting atom and the corresponding long-range stress field around it are directly related. Approximately, they can be evaluated using the continuum elastic theory of spherical or ellipsoidal inclusions developed by Eshelby[42] which is at present commonly used in the continuum theory of lattice defects.[43] Let us consider an atom at the position $\mathbf{r}_i$ such that the misfit with its surroundings leads to the local shear stress $\sigma^{\alpha\beta}(\mathbf{r}_i)$ at this atom position. By rewriting the results of Eshelby using the spherical-harmonics equivalents of stresses [Eq. (4)], it can be shown that the long-range shear stress field at a position $\mathbf{r}_j$ due to the misfit at $\mathbf{r}_i$ is

$$[\sigma_2^m(\mathbf{r}_j)]_{\mathrm{LR}}=\left[\frac{5}{14\pi}\right]^{1/2}\frac{15\Omega(-1)^m}{(7-5\nu)r_{ij}^3}\sum_{m'}\sigma_2^{m'}(\mathbf{r}_i)\left[3\begin{bmatrix}2&2&4\\-m&m'&m-m'\end{bmatrix}Y_4^{m-m'}(\hat{\mathbf{r}}_{ij})\right.$$
$$\left.-\sqrt{5}(1-\tfrac{7}{5}\nu)\begin{bmatrix}2&2&2\\-m&m'&m-m'\end{bmatrix}Y_2^{m-m'}(\hat{\mathbf{r}}_{ij})\right], \tag{16}$$

where ν is the Poisson ratio. Equation (16) represents a unique relationship between the long-range part of the stress associated with a misfitting atom i, evaluated at the position of an atom j, and the local atomic-level stress at the atom i. We show now that this relationship is the origin of the observed correlations between stresses evaluated at atoms i and j, respectively.

The long-range stress field given by Eq. (16) must lead to a stress correlation defined by Eq. (12) even when the local misfit at the atom i is not correlated with the misfit at the atom j since its value at the atom j is obviously related to the misfit at the atom i. Assuming now that the relevant stress at the atom j is only the long-range stress due to the atom i, we substitute (16) into (12) and after evaluating the summation we obtain

$$S_{i,j}^{\mathrm{LR}}(2,2,4)=\frac{3C}{\sqrt{5}r_{ij}^3}\ , \tag{17}$$

$$S_{i,j}^{\mathrm{LR}}(2,2,2)=\frac{2(5-7\nu)C}{r_{ij}^3}\ , \tag{18}$$

where

$$C=\frac{15\Omega}{\sqrt{14\pi}4\pi(7-5\nu)}\ . \tag{19}$$

The values of $S_2(n\mathrm{NN})$ and $S_4(n\mathrm{NN})$, calculated by inserting (17) and (18) into Eq. (11), are compared in Table III with those observed for $T=0$ K in the MD studies. For the nearest-neighbor correlation we also give the values of $S_l(1\mathrm{NN})$ after subtracting the high-temperature value given by Eq. (15), which represents the random state. It is seen that the MD values of $S_2(1\mathrm{NN})$ and $S_4(n\mathrm{NN})$ $(n>1)$ are well accounted for by these calculations, but other correlations found in the MD study are smaller than those calculated theoretically. These results suggest that the observed correlations arise primarily owing to the long-range stress fields produced by local misfits. However, some of the components of the stress field are strongly screened. This indicates that some structural change has apparently taken place as a consequence of the long-range stress field, and the local misfits themselves may have weak correlations.

The temperature dependence of these long-range stress fields shows that they are disrupted by thermal excitations, and completely disappear at T_s, indicating that the normal fluid above T_s cannot support this stress field. On the other hand, in the glassy state below T_g, as well as in the supercooled viscous liquid state between T_s and T_g, the long-range stress field can be supported at least partially. It is interesting to note that the temperature dependences of $S_2(1\mathrm{NN})$ and $S_4(2\mathrm{NN})$ show no anomaly at T_g, and below T_g the correlation continuously increases down to $T=0$ K without any further transition. From this point of view, the glass transition is not a

TABLE III. Spatial correlation functions $S_l(n\mathrm{NN})$ found in the molecular-dynamics calculations (MD) and evaluated using the elastic theory of misfitting atoms (EL).

nth neighbor	$S_2(n\mathrm{NN})$ MD	$S_2(n\mathrm{NN})$ EL	$S_4(n\mathrm{NN})$ MD	$S_4(n\mathrm{NN})$ EL
1	0.17	0.146	0.08	0.112
1[a]	0.10		−0.01	
2	0.005	0.028	0.027	0.022
3	0	0.008	0.007	0.006
4	0	0.004	0.005	0.003
5	0	0.002	0.001	0.001

[a]After subtracting the high-temperature value which describes the random state.

phase transition. It is likely that the increased correlations indicated by the increases in $S_2(1NN)$ and $S_4(2NN)$ and the percolation of the correlated regions lead to a glass transition, in a way similar to that proposed phenomenologically by Cohen and Grest.[44]

On the other hand, the onset of correlation at T_s might signify a more fundamental change in the structure. Above T_s the local structure is essentially uncorrelated, and the system may be regarded as a high-density gas. As temperature is reduced the stresses become correlated, and the liquid gradually develops solidlike characteristics. This itself is not surprising since as the density of gas is increased the frequency of atomic collisions increases, leading to an increase in viscosity, which in turn results in stress correlations. However, the relatively sharp onset of the correlation at T_s and the presence of selective screening of stresses indicate that the structure may be undergoing a significant change at T_s. In particular, the presence of screening implies that the system is responding to the long-range stresses and changing itself such as to accommodate the misfits in the energetically most-favorable way. This point obviously warrants further investigations.

One of the consequences of the onset of correlations at T_s is that the hydrodynamic approximation which may be valid at high temperatures, would not be justified below T_s. Hence, the assumptions currently used in the mode-coupling theory require some revisions below T_s. For instance, the random-phase approximation is usually assumed and many-particle correlation functions are decoupled into products of two-body correlation functions.[8,9] However, such procedures are not adequate below T_s since the elastic interactions lead to three- and four-body correlations. Consequences of such higher-order correlations are currently under investigation.

The present simulation was carried out using a short-range potential and keeping the volume of the system constant. The use of a longer-range potential may influence the correlations below T_s, but it is not likely to alter the nature of the correlations and their temperature dependence. The effect of keeping the volume constant is more difficult to assess, but the fact that two models with somewhat different densities showed practically identical results suggests that the effect would not be important. Nevertheless this point deserves further investigations using a constant-pressure method.[45]

VIII. CONCLUSION

A molecular-dynamics study of a model monatomic liquid was carried out in order to investigate the micromechanisms of glass transition and of the rapid increase in viscosity which leads to the glass transition. The local structure was described in terms of microscopic stresses defined at each atomic site, or the atomic-level stresses. This allows a tensorial description of the local structure, rather than the conventional scalar description in terms of the local density. The tensorial description is favored since it incorporates more realistically the atomistic nature of the interactions in the system. The present study has shown that spatial correlations among the local stresses set in at a temperature T_s which is much higher than the glass transition temperature. Below T_s various properties exhibit significant deviations from those in the liquid state. These correlations can be largely explained in terms of long-range elastic fields invoked by local misfits between the atoms and their environment which are the origin of the local atomic-level stresses, but an interesting selective screening of these stresses has been observed. This screening and a relatively sharp onset of the stress correlation may indicate some fundamental structural change at T_s, although this point needs further investigations. Percolation of such correlations and associated establishment of long-range interactions between misfitting atoms may be the origin of the glass transition.

ACKNOWLEDGMENTS

The authors are grateful to Dr. T. C. Lubensky, Dr. P. Chaikin, and Dr. S. Ramaswamy for valuable discussions. This research was supported by the National Science Foundation through the Materials Research Laboratory Program Grants No. DMR-82-16718 and No. DMR-85-19059.

*Present address: Theoretical Division, Los Alamos National Laboratory, Los Alamos, NM 87545.

[1]J. P. Hansen and I. R. McDonald, *Theory of Simple Liquids* (Academic, New York, 1986).
[2]B. J. Alder and T. E. Wainwright, Phys. Rev. Lett. **18**, 988 (1967).
[3]D. Levesque, L. Verlet, and J. Kurkijarvi, Phys. Rev. A **7**, 1690 (1973).
[4]J. J. Erpenbeck and W. W. Wood, J. Stat. Phys. **24**, 455 (1981).
[5]P. J. Steinhardt, D. R. Nelson, and M. Ronchetti, Phys. Rev. B **28**, 784 (1983).
[6]M. H. Ernst, E. H. Hauge, and J. M. J. van Leeuwen, Phys. Rev. A **4**, 2055 (1971).
[7]Y. Pomeau and P. Resibois, Phys. Rep. **19**, 63 (1975).
[8]T. Geszti, J. Phys. C **16**, 5805 (1983).
[9]U. Bengtzelius, W. Gotze, and A. Sjolander, J. Phys. C **17**, 5915 (1984).
[10]S. P. Das, G. F. Mazenko, S. Ramaswamy, and J. Toner, Phys. Rev. Lett. **54**, 118 (1985).
[11]T. R. Kirkpatrick, J. Non-Cryst. Solids **75**, 437 (1985).
[12]P. Papon and P. H. E. Meijer, Physica **101A**, 477 (1980).
[13]T. R. Kirkpatrick, Phys. Rev. A **31**, 939 (1985).
[14]P. Taborek, R. N. Kleiman, and D. J. Bishop, Phys. Rev. B **34**, 1835 (1986).
[15]T. Egami and d. Srolovitz, J. Phys. F **12**, 2141 (1982).
[16]For example, L. Landau and I. Lifshitz, *Theory of Elasticity* (Pergamon, Oxford, 1958).

[17]E. Schrödinger, Ann. Phys. (Leipzig) **82**, 265 (1927).
[18]W. Pauli, in *Handbuch der Physik* (Springer, Berlin, 1933), Vol. XXIV, Part I, p. 89.
[19]P. C. Martin and J. C. Schwinger, Phys. Rev. **115**, 1342 (1959).
[20]M. Born and K. Huang, *Dynamical Theory of Crystal Lattices* (Clarendon, Oxford, 1954).
[21]R. P. Feynman, Phys. Rev. **56**, 340 (1939).
[22]O. H. Nielsen and R. M. Martin, Phys. Rev. B **32**, 3780 (1985).
[23]For example, R. Hill, *The Mathematical Theory of Plasticity* (Clarendon, Oxford, 1950).
[24]Z. S. Basinski, M. S. Duesberry, and R. Taylor, Can. J. Phys. **49**, 2160 (1971).
[25]T. Egami, K. Maeda, and V. Vitek, Philos. Mag. A **41**, 883 (1980).
[26]D. Srolovitz, K. Maeda, V. Vitek, and T. Egami, Philos. Mag. A **44**, 847 (1981).
[27]D. Srolovitz, T. Egami, and V. Vitek, Phys. Rev. B **24**, 6936 (1981).
[28]D. Srolovitz, V. Vitek, and T. Egami, Acta Metall. **31**, 335 (1983).
[29]D. Srolovitz, K. Maeda, S. Takeuchi, T. Egami, and V. Vitek, J. Phys. F **11**, 2209 (1981).
[30]T. Egami and V. Vitek, in *Amorphous Materials: Modeling of Structure and Properties,* edited by V. Vitek (The Metallurgical Society of AIME, Warrendale, Pennsylvania, 1983), p. 127.
[31]R. A. Johnson, Phys. Rev. **A134**, 1329 (1964).
[32]D. Beeman, J. Comput. Phys. **20**, 130 (1976).
[33]M. J. L. Sangster and M. Dixon, Adv. Phys. **25**, 247 (1976).
[34]S.-P. Chen, T. Egami, and V. Vitek, in *Rapidly Quenched Metals,* edited by S. Steeb and H. Warlimont (North-Holland, Amsterdam, 1985), Vol. 1, p. 577; J. Non-Cryst. Solids **75**, 449 (1985).
[35]J. R. Wilson, Met. Rev. **10**, 381 (1965).
[36]M. Kléman and J. F. Sadoc, J. Phys. (Paris) Lett. **40**, L569 (1979).
[37]M. Kléman, in *Amorphous Materials: Modeling of Structure and Properties,* Ref. 30, p. 99.
[38]R. Mosseri and J. F. Sadoc, J. Phys. (Paris) Lett. **45**, L827 (1984).
[39]D. R. Nelson, Phys. Rev. B **28**, 5515 (1983).
[40]S. Sachdev and D. R. Nelson, Phys. Rev. Lett. **53**, 1947 (1984).
[41]T. Egami, J. Mater. Sci. **13**, 2589 (1978).
[42]J. D. Eshelby, Proc. R. Soc. London, Ser. A **153**, 376 (1957).
[43]C. Teodosiu, *Elastic Models of Crystal Defects* (Springer, Berlin, New York, 1982).
[44]M. H. Cohen and G. S. Grest, Phys. Rev. B **20**, 1077 (1979).
[45]H. C. Anderson, J. Chem. Phys. **72**, 2384 (1980).